# Statistical Hydrodynamics in Trickle Flow Columns

**M. Crine, P. Marchot, and G. L'Homme**
Laboratoire de génie chimique, Institut de Chimie-B6, Université de Liège, B-4000 Liège, Belgium

*A stochastic model is proposed for the description of the hydrodynamics in trickle flow columns. The gas-liquid flow is assumed to be controlled by local packing properties which are represented by random variables. The first (microscopic) level of description corresponds to the smallest volume whose averaged geometrical properties are representative of the whole packing. The hydrodynamics at this level is described by Ergun equations. The second level describes the liquid flow maldistribution induced by the partial wetting of the solid. This is the macroscopic level where the hydrodynamics is described by a probability distribution. This approach is used to develop correlations for predicting the wetting efficiency, the dynamic liquid holdup, and the pressure drop. These correlations give very good results when compared to experimental data over a wide range of operating conditions. In addition, we propose to describe the hysteretic behavior of trickle beds by a modification of the liquid flow texture caused by different values of the apparent solid wettability.*

## Introduction

Several methods have been proposed to model hydrodynamical processes in trickle flow columns. Most of them are based on empirical correlations using dimensional analysis and a wide range of experimental data. Some theoretical approaches reported recently may be grouped into two main categories, depending on the technique adopted to extend to the bed scale the description of gas-liquid-solid interactions occurring at the particle scale.

The first group involves models based on deterministic methods. They consist of averaging the flow equations governing the fluid flow at the particle scale by an analytical integration over a defined volume element. These macroscopic equations are derived by applying volume-averaging techniques as described by Whitaker (1969), Slattery (1972), and Brenner (1980). The averaged equations are presented in such a way that they involve only macroscopic quantities having a physical meaning at the bed scale (such as averaged holdups and flow rates). These techniques have been applied to the modeling of diverse multiphase systems: Zanotti and Carbonell (1984), Grosser et al. (1988), and Dankworth et al. (1990).

The volume over which the equations have to be averaged must be large enough to include all the spatial velocity fluctuations, which we consider as occurring at the local level. From this viewpoint, the size and the geometry of the volume elements are fixed primarily by the packing texture. The selection of a representative geometry is not an easy task since the real geometry is very complex. In most cases, simple geometries as capillary tubes are adopted. The main drawback of such simple representations is that they completely overlook the problem of liquid flow maldistribution which may be observed experimentally at a much larger scale than the particle one (Hoek et al. 1986; Crine, 1988; Crine et al., 1991). These velocity fluctuations result from the random distribution of the liquid flow paths in the bed. They directly control the partial wetting of the solid (Crine, 1988; Marchot, 1988). This means that the size of the volume element, over which these fluctuations could be averaged, should depend on the wetting efficiency and, in turn, on the operating conditions.

The current deterministic approach does not seem to be well adapted to account for the complexity and the randomness of the liquid flow distribution in a packed bed. That is certainly one of the reasons why the volume-averaging techniques have never been able to describe correctly the partial wetting in a trickle flow column nor its dependence on the operating conditions. As a matter of fact, no correlation of the wetting efficiency using averaged equations has ever been proposed in the literature. Moreover, most of the recent applications of averaged equations deal with large gas and liquid flow rates for which the wetting is nearly complete (Grosser et al., 1988; Dankworth et al., 1990).

The second group of models is based on a probabilistic approach. This method was introduced by Matheron (1966). It has been applied extensively to the morphological analysis of porous media. In previous articles, we have shown how it may also be applied to the description of the liquid flow distribution in a packed bed by means of the concept of percolation: Crine (1978, 1988), Crine et al. (1979), Marchot (1988), and Marchot et al. (1987).

The liquid flow distribution is considered as resulting from the interactions between the fluids and the porous texture. The packing properties governing these interactions are called accessibility properties. They vary in such a complex manner that they must be considered as random variables, which we can describe partially by means of a probabilistic approach. These considerations have led us to introduce the concept of statistical hydrodynamics.

This concept assumes that all the local hydrodynamical quantities (such as fluid holdups and flow rates, and wetting efficiency) may be considered as random variables, like the packing properties. The main problem thus resides in determining the probability distributions and the averaged values of these variables at the bed scale. We will consider that these random variables must be statistically homogeneous, that is, *ergodic* and *stationary*. This assumption is adopted commonly when analyzing porous media (Matheron, 1966). This approach *per se* is also based on a volume-averaging technique. It introduces two levels of modeling:

- The microscopic level, the level of a few particles
- The macroscopic level, the level of the whole bed or of a volume large enough to be representative of the whole bed.

At the microscopic level, the hydrodynamics results from local interactions among the gas, liquid and solid phases (mass, energy and momentum transports). The relevant hydrodynamical quantities may be determined by a model describing these interactions at the level of the particles. The change of scale between the microscopic and macroscopic levels may be achieved by averaging the local quantities weighted by a probability distribution describing the random nature of the phenomena.

This methodology may be applied to the modeling of any type of hydrodynamical processes. In this article, we will illustrate applications to the modeling of three quantities directly affected by the quality of distribution of the fluids in the packed bed: the wetting efficiency, the dynamic liquid holdup, and the pressure drop.

## Modeling at the Microscopic Level

The description of the local interactions among the gas, the liquid and the particles requires the choice of an elementary cell. This cell may be characterized as the smallest volume element whose locally averaged geometrical properties are stationary, that is, uniformly distributed in the bed. If the packing is statistically homogeneous, the characteristic size of the elementary cell will be close, but always larger than the particle size (Oger et al., 1989). This characteristic size defines the microscopic level. One may note that to avoid any confusion between this microscopic level and the level of one individual particle, the scale of the elementary cell is sometimes called the mesoscopic level.

The hydrodynamics in the elementary cell may be described by a constitutive equation such as the Ergun equation (Ergun, 1952). Because of the stationary properties of the elementary cell, the coefficients of the Ergun equation ($A$ and $B$ in Eqs. 1 and 2) are representative of the whole packing.

We will consider here the regime of low gas-liquid interactions, as defined by Specchia and Baldi (1977). This flow regime has been called the "geometrical interaction" regime by Rao and Drinkenburg (1985). Each fluid is "seen" by the other as an extension of the solid phase. This clearly corresponds to the case of low gas-liquid interactions. It is then rather easy to apply the Ergun equation to describe the gas and the liquid flows in the packed bed. The total void fraction $\epsilon$, which classically appears in the Ergun equation, has to be replaced by the dynamic liquid holdup $\epsilon_d$ for the liquid phase and by $\epsilon-\epsilon_d-\epsilon_S$ for the gaseous phase. $\epsilon_S$ represents the static liquid holdup, that is, the volume fraction of liquid that remains in the bed when there is no more liquid flow. The Ergun equation may then be written for the two phases:

$$-\frac{dP_G}{dx}+\rho_G g=\left[A\frac{(1-\epsilon+\epsilon_d+\epsilon_S)^2}{(\epsilon-\epsilon_d-\epsilon_S)^3}\frac{Re_G}{Ga_G}+B\frac{1-\epsilon+\epsilon_d+\epsilon_S}{(\epsilon-\epsilon_d-\epsilon_S)^3}\frac{Re_G^2}{Ga_G}\right]\rho_G g \quad (1)$$

$$-\frac{dP_L}{dx}+\rho_L g=\left[A\frac{(1-\epsilon_d)^2}{\epsilon_d^3}\frac{Re_L}{Ga_L}+B\frac{1-\epsilon_d}{\epsilon_d^3}\frac{Re_L^2}{Ga_L}\right]\rho_L g \quad (2)$$

We should note that this set of local constitutive equations, based on the Ergun equation and on the assumption of geometrical interactions, could be easily replaced by any other sets of constitutive models.

Equations 1 and 2 may be related to the relative permeability concept developed by Sáez and Carbonell (1985). The relative permeabilities $k_L$ and $k_G$ for the liquid and gas phases are indeed defined as the ratio between the pressure drops (including the gravity effect) in single-phase flow and two-phase flow, respectively.

$$k_L=\frac{\left[A\frac{(1-\epsilon)^2}{\epsilon^3}\frac{Re_L}{Ga_L}+B\frac{1-\epsilon}{\epsilon^3}\frac{Re_L^2}{Ga_L}\right]}{\left[A\frac{(1-\epsilon_d)^2}{\epsilon_d^3}\frac{Re_L}{Ga_L}+B\frac{1-\epsilon_d}{\epsilon_d^3}\frac{Re_L^2}{Ga_L}\right]} \quad (3)$$

$$k_G=\frac{\left[A\frac{(1-\epsilon)^2}{\epsilon^3}\frac{Re_G}{Ga_G}+B\frac{1-\epsilon}{\epsilon^3}\frac{Re_G^2}{Ga_G}\right]}{\left[A\frac{(1-\epsilon+\epsilon_d+\epsilon_S)^2}{(\epsilon-\epsilon_d-\epsilon_S)^3}\frac{Re_G}{Ga_G}+B\frac{1-\epsilon+\epsilon_d+\epsilon_S}{(\epsilon-\epsilon_d-\epsilon_S)^3}\frac{Re_G^2}{Ga_G}\right]} \quad (4)$$

Because the Reynolds and Galileo numbers appear both in the denominators and numerators of these equations, $k_L$ and $k_G$ depend essentially on the volume fractions occupied by the fluids. $k_L$ tends to 1 as the liquid fills all the voids between the particles ($\epsilon_d=\epsilon-\epsilon_S$). $k_G$ tends to a value slightly smaller than 1 for the gaseous phase because of the static holdup $\epsilon_S$ remaining in the bed when the liquid flow rate is equal to 0 ($\epsilon_d=0$).

The equality of the pressure drop in the gaseous and liquid

phases, coupled with Eqs. 1 and 2, yields a system of two equations with two unknowns: the dynamic liquid holdup $\epsilon_d$ and $\psi_L$, the dimensionless pressure drop of the liquid phase including the gravity effects, defined by:

$$\psi_L = \frac{(-dP_L/dx + \rho_L g)}{\rho_L g} \tag{5}$$

It follows then (considering $\rho_L \gg \rho_G$):

$$\frac{\rho_L}{\rho_G}(\psi_L - 1) = \left[ A \frac{(1-\epsilon+\epsilon_d+\epsilon_S)^2}{(\epsilon-\epsilon_d-\epsilon_S)^3} \frac{Re_G}{Ga_G} + B \frac{1-\epsilon+\epsilon_d+\epsilon_S}{(\epsilon-\epsilon_d-\epsilon_S)^3} \frac{Re_G^2}{Ga_G} \right] \tag{6}$$

$$\psi_L = \left[ A \frac{(1-\epsilon_d)^2}{\epsilon_d^3} \frac{Re_L}{Ga_L} + B \frac{1-\epsilon_d}{\epsilon_d^3} \frac{Re_L^2}{Ga_L} \right] \tag{7}$$

These two equations define completely the hydrodynamics at the particle or local scale. They allow us to calculate $\epsilon_d$ and $\psi_L$, provided that we know the local operating conditions ($Re_G$ and $Re_L$), the fluid properties ($Ga_G$ and $Ga_L$) and the static holdup ($\epsilon_S$). The latter may be determined independently using such correlation as the one reported by Sáez and Carbonell (1985).

$$\epsilon_S = 1 \Big/ \left[ 20 + 0.9 \frac{\epsilon^2}{(1-\epsilon)^2} E_{oL} \right] \tag{8}$$

where the Eötvos number $Eo_L$ is defined as:

$$Eo_L = \frac{\rho_L g d_p^2}{\sigma_L} \tag{9}$$

Let us note that Eqs. 6 and 7 have been developed at the microscopic level (at the level of the elementary cell). They do not account for the effect of the random distribution of the liquid flow paths and of the partial wetting of the solid. This will be introduced at the macroscopic level.

## Modeling at the Macroscopic Level

### *Flow Rate Distribution*

The random distribution of the accessibility properties of the packing generates interconnections between the elementary cells defined at the microscopic level. A random distribution of the gas and liquid flow paths results from these interconnections whose characteristic length is much larger than the size of the elementary cell (Oger et al., 1989). This new characteristic length characterizes the minimum volume over which averaged hydrodynamic quantities are representative of the whole packing hydrodynamics. This will be called the macroscopic level.

The random liquid flow rate distribution at this level may be represented by a percolation model (Crine, 1978, 1988; Crine et al., 1979; Marchot et al., 1987; Marchot, 1988). The maximum entropy principle allows the determination of the following probability distribution:

$$p(Re_{L,i}) = \exp(c + d\, Re_{L,i}/Re_{\min}) \tag{10}$$

$$\text{for } Re_{L,i} = 0,\ Re_{\min},\ \ldots,\ iRe_{\min},\ \ldots,\ Re_{\max}$$

$p(Re_{L,i})$ represents the probability of observing, a local liquid flow rate characterized by the local Reynolds number $Re_{L,i}$. $Re_{\max}$ and $Re_{\min}$ represent the maximum and minimum values that the local liquid Reynolds number can take. The former corresponds to a local liquid flooding of the packing. The latter corresponds to the minimum energy necessary for the liquid to wet the solid. It represents thus the minimum value, below which there is no more liquid flow and, consequently, no more wetting and liquid holdup. The physical meaning and the way to calculate these values are as follows.

The constants $c$ and $d$ in Eq. 10 are determined by two constraints: the sum of probabilities must equal 1:

$$\sum_{Re_{L,i}=0}^{Re_{\max}} p(Re_{L,i}) \frac{\Delta Re_{L,i}}{Re_{\min}} = 1 \tag{11}$$

and the mean liquid flow rate is imposed by the averaged value of the Reynolds number at the bed scale $\langle Re_L \rangle$.

$$\sum_{Re_{L,i}=0}^{Re_{\max}} Re_{L,i}\, p(Re_{L,i}) \frac{\Delta Re_{L,i}}{Re_{\min}} = \langle Re_L \rangle \tag{12}$$

The discretization step $\Delta Re_{L,i}$ does not affect significantly the integrations, provided that the ratio $\Delta Re_{L,i}/Re_{\min}$ is smaller than 0.2 (Crine, 1988). Very often, the maximum Reynolds number $Re_{\max}$ is much larger than the minimum Reynolds number $Re_{\min}$. In this case, the constant $d$ in Eq. 10 is negative, and the probability distribution exhibits an exponential decrease vs. the local liquid flow rate. This dependence is confirmed by many experimental findings reported in the literature (Hoek et al. 1986; Crine, 1988; Crine et al., 1991).

### *Averaging Formulas*

The liquid flow in each of the elementary cells is characterized by a local Reynolds number $Re_{L,i}$. The local gas Reynolds number $Re_{G,i}$ and the local dynamic liquid holdup $\epsilon_{d,i}$ may be computed by Eqs. 6 and 7, if we impose the pressure drop $\psi_L$.

$$\frac{\rho_L}{\rho_G}(\psi_L - 1) = \left[ A \frac{1-\epsilon+\epsilon_{d,i}+\epsilon_S)^2}{(\epsilon-\epsilon_{d,i}-\epsilon_S)^3} \frac{Re_{G,i}}{Ga_G} + B \frac{1-\epsilon+\epsilon_{d,i}+\epsilon_S}{(\epsilon-\epsilon_{d,i}-\epsilon_S)^3} \frac{Re_{G,i}^2}{Ga_G} \right] \tag{13}$$

$$\psi_L = \left[ A \frac{(1-\epsilon_{d,i})^2}{\epsilon_{d,i}^3} \frac{Re_{L,i}}{Ga_L} + B \frac{1-\epsilon_{d,i}}{\epsilon_{d,i}^3} \frac{Re_{L,i}^2}{Ga_L} \right] \tag{14}$$

Furthermore, according to the definition of the minimum Reynolds number, the local wetting efficiency $f_{w,i}$ is null below $Re_{\min}$ and equal to 1 above (complete local wetting).

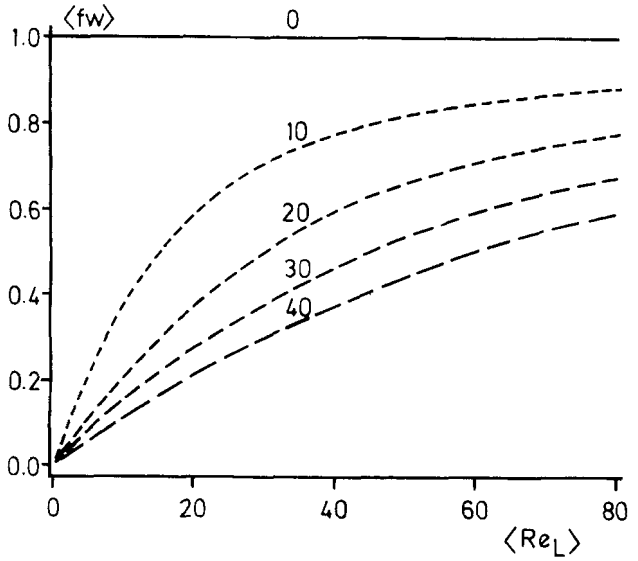


**Figure 1. Dependence of the wetting efficiency $\langle f_w \rangle$ on the liquid Reynolds number $\langle Re_L \rangle$ for conditions in Table 1.**

Parameter is $Re_{min}$.

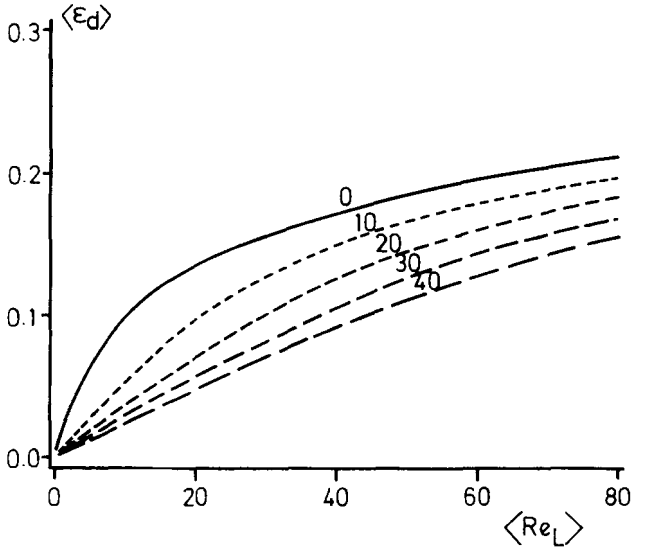


**Figure 2. Dependence of the dynamic liquid holdup $\langle \epsilon_d \rangle$ on the liquid Reynolds number $\langle Re_L \rangle$ for conditions in Table 1.**

Parameter is $Re_{min}$.

$$f_{w,i} = \begin{cases} 1 \text{ for } Re_{L,i} \geq Re_{\min} \\ 0 \text{ for } Re_{L,i} < Re_{\min} \end{cases} \tag{15}$$

The corresponding macroscopic quantities may then be determined by the following averaging formulas.

$$\langle Re_G \rangle = \sum_{Re_{L,i}=0}^{Re_{\max}} Re_{G,i}\, p(Re_{L,i})\, \frac{\Delta Re_{L,i}}{Re_{\min}} \tag{16}$$

$$\langle \epsilon_d \rangle = \sum_{Re_{L,i}=0}^{Re_{\max}} \epsilon_{d,i}\, p(Re_{L,i})\, \frac{\Delta Re_{L,i}}{Re_{\min}} \tag{17}$$

$$\langle f_w \rangle = \sum_{Re_{L,i}=0}^{Re_{\max}} f_{w,i}\, p(Re_{L,i})\, \frac{\Delta Re_{L,i}}{Re_{\min}} \tag{18}$$

The relations 16 to 18, coupled with the constraint equations (Eqs. 11 and 12), form a set of five equations, in which the local parameters are determined by the probability distribution (Eq. 10) and by the hydrodynamics at the microscopic level (Eqs. 13 to 15). There remain five unknowns: the macroscopic wetting efficiency $\langle f_w \rangle$, the macroscopic liquid holdup $\langle \epsilon_d \rangle$, the pressure drop $\psi_L$, and the two constants $c$ and $d$ of the probability distribution.

The resolution of these five equations allows the calculation of the macroscopic hydrodynamical quantities in relation to the macroscopic flow rates $\langle Re_L \rangle$ and $\langle Re_G \rangle$. These relationships are illustrated in Figures 1 and 2 for the parameter values listed in Table 1. These figures refer to a zero gas flow rate. In the regime of low gas-liquid interactions, the influence of the gas flow rate is weak and may often be neglected. If not, this influence may be accounted for by means of Eq. 13. In any case, the wetting efficiency $\langle f_w \rangle$ and the liquid holdup $\langle \epsilon_d \rangle$ are increasing functions of the Reynolds number $\langle Re_L \rangle$. The wetting efficiency reaches unity asymptotically as the Reynolds number tends to infinity. This corresponds fairly well to a large diversity of experimental observations correlated, for example, by the relation proposed by Puranik and Vogelpohl (1974).

Figures 1 and 2 explain the role of wetting parameter played by the minimum Reynolds number $Re_{min}$. Indeed, both $\langle f_w \rangle$ and $\langle \epsilon_d \rangle$ decrease as $Re_{min}$ increases, when the solid surface is more difficult to wet. The shape of the curves is also modified. For instance, the exponent of a power fit of $\langle \epsilon_d \rangle$ vs. $\langle Re_L \rangle$ equals approximately 1/3 when $Re_{min}$ equals 0. This corresponds to a completely developed laminar film. As $Re_{min}$ increases, the apparent log-slope increases up to approximately 0.7 for $Re_{min} = 40$. This evolution is confirmed by many experimental results which show that the exponent of the power fit of $\langle \epsilon_d \rangle$ increases as the wetting of the solid is decreased. This has been interpreted by Charpentier et al. (1968) as a transition between a film and a rivulet flow.

The set of equations described above allows also the *a posteriori* determination of the macroscopic relative permeabilities $\langle k_L \rangle$ and $\langle k_G \rangle$ defined by:

$$\langle k_L \rangle = \frac{\left[ A \dfrac{(1-\epsilon)^2}{\epsilon^3} \dfrac{\langle Re_L \rangle}{Ga_L} + B \dfrac{1-\epsilon}{\epsilon^3} \dfrac{\langle Re_L \rangle^2}{Ga_L} \right]}{\psi_L} \tag{19}$$

**Table 1. Parameter Values and Operating Conditions for Simulations in Figures 1, 2 and 3**

| | | | | | |
|---|---|---|---|---|---|
| $\epsilon$ | = | 0.35 | $Ga_L$ | = | $10^6$ |
| $\epsilon_S$ | = | 0.05 | $Ga_G$ | = | $5.10^4$ |
| $A$ | = | 180 | $\langle Re_G \rangle$ | = | 0.0 |
| $B$ | = | 1.8 | $\langle Re_L \rangle$ | = | 0.0 – 80.0 |
| | | | $Re_{min}$ | = | 0.0 – 40.0 |
| | | | $Re_{max}$ | = | $1.10^4$ |

$$\langle k_G \rangle = \frac{\left[ A \frac{(1-\epsilon)^2}{\epsilon^3} \frac{\langle Re_G \rangle}{Ga_G} + B \frac{1-\epsilon}{\epsilon^3} \frac{\langle Re_G \rangle^2}{Ga_G} \right]}{\frac{\rho_L}{\rho_G} (\psi_L - 1)} \quad (20)$$

The relation between $\langle k_L \rangle$ and the liquid saturation $\langle \epsilon_d \rangle / (\epsilon - \epsilon_S)$ is shown in Figure 3 for the same conditions as adopted in Figures 1 and 2. As might be expected, $\langle k_L \rangle$ is an increasing function of the liquid saturation.

Sáez and Carbonnel (1985) proposed a power fit of relative liquid permeability vs. the liquid saturation, based on data taken from the literature. They obtained an exponent equal to 2.43. Later on, Levec et al. (1986) proposed different values ranging between 2 and 2.9. The most important information to be drawn from those empirical laws is that the exponent is always smaller than the theoretical value it should take at the microscopic level.

At the microscopic level, the power fit of Eq. 3 yields indeed exponent values a little bit greater than 3 (between 3 and 3.5). Sáez et al (1986) arrived at similar results with a capillary tube model, which accounts for the packing geometry only at the particle scale.

This difference between microscopic and macroscopic results may be interpreted in terms of imperfect wetting of the packing. The exponents of power fits of the curves represented in Figure 3 decrease as the minimum Reynolds number $Re_{min}$ increases. For the cases in Figure 3, this exponent decreases from approximately 3.5 ($Re_{min} = 0$) to 1.5 ($Re_{min} = 40$). This means that the apparent exponent increases with the solid wetting and with the liquid saturation. This agrees with the findings of Levec et al. (1986), who proposed an exponent of 2.0 for a liquid saturation smaller than 0.2 and 2.9 above 0.2.

It is instructive to note that, for a given liquid saturation, the relative permeability $\langle k_L \rangle$ increases with the minimum Reynolds number $Re_{min}$. For a small value of $Re_{min}$, the wetting is nearly complete and the liquid is mainly in the form of films covering almost all the solid surface. This leads to a large amount of gas-liquid interfacial interactions and results in high-pressure drops corresponding to low values of $\langle k_L \rangle$. As $Re_{min}$ increases, the wetting is reduced, and progressively the liquid flow takes the form of isolated rivulets (Crine et al., 1981a). This segregated gas-liquid flow results in less important interactions and thus lower pressure drops. This corresponds to larger values of $\langle k_L \rangle$. The existence of these different textures of liquid flow and their effect on the pressure drop have been reported in the literature (Christensen et al., 1986; Chu and Ng, 1989).

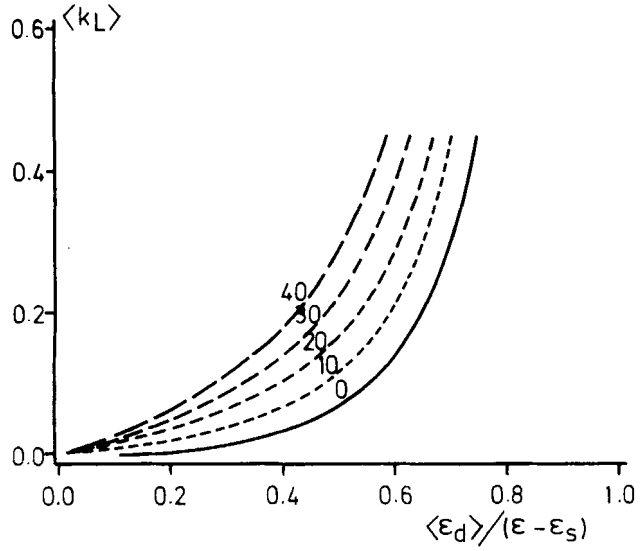


**Figure 3. Dependence between the macroscopic liquid relative permeability $\langle k_L \rangle$ and the liquid saturation $\langle \epsilon_d \rangle / (\epsilon - \epsilon_S)$ for conditions in Table 1.**

Parameter is $Re_{min}$.

### *Maximum Reynolds Number*

The use of the flow rate distribution law (Eq. 10) requires the values of $Re_{min}$ and $Re_{max}$. The latter corresponds to a local flooding of the packed bed, that is, to a local liquid holdup $\epsilon_{max}$ equal to the total void fraction $\epsilon$ minus the static liquid holdup $\epsilon_S$. $Re_{max}$ may thus be determined using Eq. 14, in which we let the local liquid holdup equal $\epsilon - \epsilon_S$.

$$\psi_L = \left[ A \frac{(1-\epsilon+\epsilon_S)^2}{(\epsilon-\epsilon_S)^3} \frac{\mathrm{Re}_{max}}{Ga_L} + B \frac{1-\epsilon+\epsilon_S}{(\epsilon-\epsilon_S)^3} \frac{Re_{max}^2}{Ga_L} \right] \quad (21)$$

This Reynolds number is an increasing function of the Galileo number $Ga_L$ (the particle size), of the pressure drop $\psi_L$ (gas flow rate) and of the packing void fraction $\epsilon$.

The maximum Reynolds number $Re_{max}$ may affect the hydrodynamics in two ways:

- By narrowing the flow rate range between $Re_{min}$ and $Re_{max}$ in which the liquid flow rate may fluctuate.
- By imposing a maximum value for the macroscopic Reynolds number $\langle Re_L \rangle$, above which there is a total flooding of the whole packed bed.

The effect of $Re_{max}$ depends thus on both the particle wettability (the value of $Re_{min}$) and the range of the liquid flow rate. To illustrate this effect, let us consider two limit examples.

The first example concerns large-size particles with high void fraction, as often encountered in distillation columns or gas-liquid absorption towers. Let us take a void fraction equal to 0.7 and a Galileo number $Ga_L$ equal to $6.10^7$. In this case, Eq. 21 yields an $Re_{max}$ greater than 6,200 for a pressure drop $\psi_L$ equal to 1. The values of parameters $A$ and $B$ in the Ergun equation are those adopted in Figures 1 to 3. Such a result is significantly above the usual range of values for $Re_{min}$ and $\langle Re_L \rangle$. The influence of $Re_{max}$ is thus negligible.

The second example concerns packings of small particles ($d_p \approx 1$ mm) with a rather small void fraction ($\epsilon \approx 0.3$). These conditions often prevail in catalytic trickle bed reactors. Let us take a Galileo number equal to 8,000. In this case, $Re_{max}$ equals approximately 7, still for a pressure drop $\psi_L$ equal to 1. This value is much closer to the usual values of $Re_{min}$ and $\langle Re_L \rangle$. This means that the local liquid flooding may significantly affect the hydrodynamics especially in packings of very small particles and high density.

### *Minimum Reynolds Number*

The minimum Reynolds number is associated with the minimum liquid flow rate ensuring a stable flow on the packing surface. The stability of a liquid film trickling over a solid surface has motivated a lot of experimental and theoretical work. In our study, we deal with the stability phenomenon at low Reynolds numbers where the wetting properties of the solid play an essential role. This problem is critical in heat exchangers in which the occurrence of dry patches may lead

to the formation of hot spots and eventually to the runaway of the apparatus. Most of the work carried out in this field has been focused on the operation of nuclear power plants (Hartley and Murgatroyd, 1964; Bankoff, 1971). The different attempts to model this phenomenon by the methods of hydrodynamical instabilities have been unsuccessful (Bankoff, 1971; Mikielewicz and Moszynski, 1976). The perturbation techniques used to treat this problem concern indeed a liquid flow covering the entire surface of the packing. The competition between the gaseous and liquid phases to contact the solid is completely ignored.

The two first attempts to account for this competition have been reported nearly simultaneously by Hartley and Murgatroyd (1964) and Hobler (1964). The first one is based on a equilibrium of forces at the stagnation line between the wetted and dry areas, whereas the second is based on a minimization of the energy dissipated to ensure a stable liquid flow on the solid surfaces. Both criteria assume planar surfaces: they neglect any curvature effect.

In many cases, this assumption is not correct, especially when the size of the particles is small. Wijffels et al. (1974) have proposed another criterion that accounts for this effect by assuming that the ratio between the gas-liquid and liquid-solid interfacial area is a linear decreasing function of $\epsilon_d/\epsilon$. [This ratio was called liquid saturation by Wijffels et al. (1974). This is slightly different from the definition we have adopted in Figure 3.]

$$\frac{a_{GL}}{a_{LS}} = 1 - \frac{\epsilon_d}{\epsilon} \tag{22}$$

The decrease of $a_{GL}$ reduces the energy necessary to create the gas-liquid interface. The effect is increased as the particle size decreases. Adopting an approach based on the minimization of the energy, Wijffels and coworkers derived the following equation:

$$\left(C_e \frac{\epsilon}{6(1-\epsilon)} \frac{Eo_L}{Ga_L} \frac{Re^2_{\min}}{\epsilon^2_{\min}} + 1\right) \frac{\epsilon_{\min}}{\epsilon} = \frac{1}{1-\alpha} \frac{Eo_L}{Eo_S} \tag{23}$$

$\epsilon_{\min}$ represents the local dynamic liquid holdup corresponding to a local Reynolds number equal to $Re_{\min}$. The constant $C_e$ equals to the ratio between the mean square velocity and the square of the mean velocity in the liquid film. The introduction of this parameter avoids unnecessary details about the shape of the velocity profiles in the liquid films.

The parameter $\alpha$ represents the apparent exponent of the relationship between the dynamic liquid holdup $\epsilon_d$ and the Reynolds number $Re_L$.

$$\alpha = \frac{Re_L}{\epsilon_d} \frac{\partial \epsilon_d}{\partial Re_L} \tag{24}$$

This exponent as well as the holdup $\epsilon_{\min}$ may be determined using the equations ruling the hydrodynamics at the microscopic level (Eqs. 1 and 2). $\alpha$ may vary between 0.3 and 0.5 depending on the importance of the turbulent contribution. For a laminar flow on planar surfaces, the exponent is equal to 1/3.

$Eo_L$ is the classical Eötvos number for the liquid phase. $Eo_S$ is a modified Eötvos number, in which the surface tension is replaced by the superficial energy $E_S$ referred to the unit area of solid.

$$Eo_S = \frac{\rho_L g d_p^2}{E_s} \tag{25}$$

$E_S$ is related to the contact angle by:

$$E_S = \sigma_L(1 - \cos\theta) \tag{26}$$

The ratio $Eo_L/Eo_S$ may then be related to the contact angle $\theta$ by:

$$\frac{Eo_L}{Eo_S} = 1 - \cos\theta \tag{27}$$

The lefthand side of Eq. 23 involves two terms that contribute to the liquid film stability. The term in $Re^2_{\min}$ represents the contribution of the kinetic energy to the spreading of the liquid film. The term in $\epsilon_{\min}$ represents the contribution of the liquid holdup that reduces the gas-liquid interfacial area $a_{GL}$ (Eq. 22), and consequently, the superficial energy $E_S$ referred to the unit area of solid. The relative importance of these two terms depends strongly on the operation conditions, especially the particle size and the packing void fraction.

With large particles and/or high void fraction, the term in $Re^2_{min}$ is predominant. Equation 23 becomes then:

$$\frac{C_e}{6(1-\epsilon)} \frac{Re^2_{\min}}{\epsilon_{\min}} = \frac{Ga_L}{(1-\alpha)Eo_S} \tag{28}$$

If, furthermore, we assume a laminar flow over planar surfaces, we obtain:

$$Re_{\min} = \left(\frac{9}{C_e}\right)^{3/5} (1-\epsilon)^{3/5}\, Ga_L^{2/5}\, Eo_S^{-3/5}\, \psi_L^{-1/5} \tag{29}$$

It is quite similar to the Hartley and Hobler criteria. It exhibits for $Re_{\min}$ a marked dependence on the liquid viscosity ($\propto \mu_L^{-4/5}$) and the superficial energy ($\propto E_S^{3/5}$), but no dependence on the particle diameter.

With small particles and/or void fraction, the term in $Re^2_{\min}$ becomes negligible. The liquid film stability is essentially defined by the decrease of the gas-liquid interfacial area $a_{GL}$. The term in $\epsilon_{\min}$ is predominant. Equation 23 becomes then:

$$\epsilon_{\min} = \frac{\epsilon}{1-\alpha} \frac{Eo_L}{Eo_S} \tag{30}$$

The Reynolds number $Re_{\min}$ that corresponds to a liquid holdup $\epsilon_{\min}$ may be determined by Eq. 7. If, once again, we assume a laminar flow over planar surfaces, Eq. 30 may be rewritten as follows:

$$Re_{\min} \approx A^{-1} \left(\frac{\epsilon}{1-\alpha}\right)^3 \left(\frac{Eo_L}{Eo_S}\right)^3 Ga_L\, \psi_L \tag{31}$$

Under this form, the criterion of Wijffels et al. exhibits for

Table 2. Parameter Estimates Corresponding to Porous Particles ($\langle Re_L \rangle$ = 0 – 35; $\langle Re_G \rangle$ = 0 – 10)

| Reference | Symbol | Particle dia. | Porosity | Liquid | $A$ | $B$ | $Re_{min}$ |
|---|---|---|---|---|---|---|---|
| Sicardi et al. (1981) | □ | 0.1 cm | 0.41 | Water | 192 | 5 | 0.6 |
| Colombo et al. (1976) | □ | 0.1 cm | 0.36 | Water | 189 | 5 | 0.3 |
| Herskowitz (1978) | □ | 0.16 cm | 0.38 | α Methylstyrene | 180 | 1.8 | 0.3 |
| Mata and Smith (1981) | □ | 0.23 cm | 0.41 | Water | 180 | 1.8 | 1.6 |
| Colombo et al. (1976) | □ | 0.41 cm | 0.41 | Water | 243 | 1.3 | 1.7 |

$Re_{min}$ a strong dependence on the particle size ($\propto d_p^3$), the solid wettability [$\propto(1-\cos\theta)^3$], and the liquid viscosity ($\propto \mu_L^{-2}$). Actually, $Re_{min}$ decreases with any modification that causes an increase of the liquid saturation, that is, a decrease of the interfacial area $a_{GL}$.

## Comparison with Experiments

The experimental data to which the model may be compared are very diverse. They consist mainly of dynamic liquid holdup, wetting efficiency, and pressure drop measurements. The results of these experiments depend not only on the ranges of gas and liquid flow rates, but also on the size, the shape and the nature of the solid particles. To analyze a wide range of operating conditions, we will consider data coming from three main fields of activity:

- The laboratory-scale catalytic trickle-bed reactors: the catalyst particles are small porous granules, whereas the gas and liquid flow rates are small ($\langle Re_L \rangle$) and $\langle Re_G \rangle \leq 10$)
- The laboratory-scale trickle-bed columns used for hydrodynamic studies: the particles—similar in shape and size to the catalyst particles—are often nonporous, whereas the gas and liquid flow rates are larger ($\langle Re_L \rangle$ and $\langle Re_G \rangle \leq 150$)
- The gas-liquid absorption columns: the nonporous hollow particles have rather complex shapes and much larger sizes, whereas the gas and liquid flow rates are similar to the preceeding case ($\langle Re_L \rangle$ and $\langle Re_G \rangle \leq 150$).

### *Data Analysis*

For these different types of application, we will limit our analysis to the regime of low gas-liquid interactions because our model has been developed for this situation. The hydrodynamic model (Eqs. 11, 12, and 16 to 18) has been fitted to these data by means of three parameters: coefficients $A$ and $B$ of the Ergun equation and the minimum Reynolds number $Re_{min}$.

*Porous Particles in Trickle-Bed Reactors.* Most of numerous data reported in the literature concerning hydrodynamic properties of catalytic trickle-bed reactors have been analyzed in important reviews (Shah, 1979; Smith et al., 1987). These data involve measurements of the dynamic liquid holdup, the pressure drop, and the wetting efficiency, although the first two are much more numerous. The sources and types of data, together with the parameter estimates, are presented in Table 2. The agreement between predicted and experimental values is shown in Figures 4 to 6.

The determination of coefficients $A$ and $B$ requires experimental data on the dynamic liquid holdup or the pressure drop. Both parameters appear indeed only in the equations involving these two experimental variables. In the absence of such information (Herskowitz, 1978; Mata and Smith, 1981), $A$ and $B$ have been fixed to the values proposed by Macdonald et al. (1979), that is, 180 and 1.8, respectively.

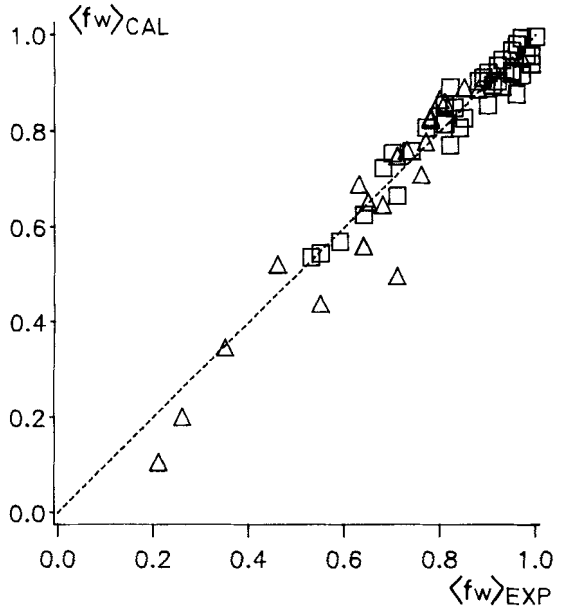


Figure 4. Comparison of predicted and experimental wetting efficiencies: symbols refer to Tables 2 to 4.

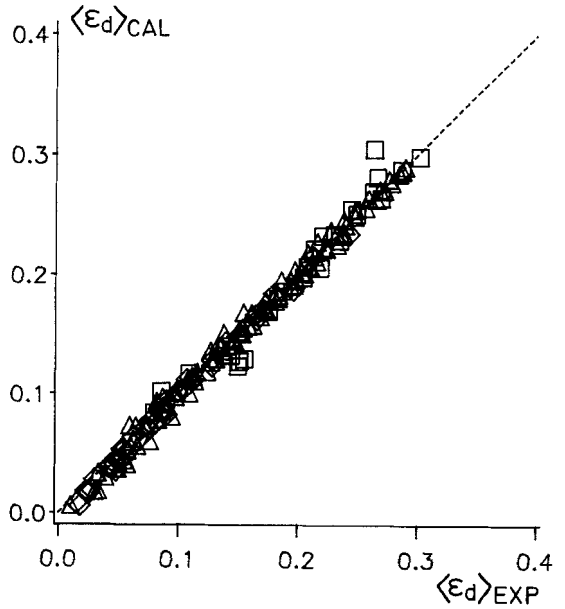


Figure 5. Comparison of predicted and experimental dynamic liquid holdups: symbols refer to Tables 2 to 4.

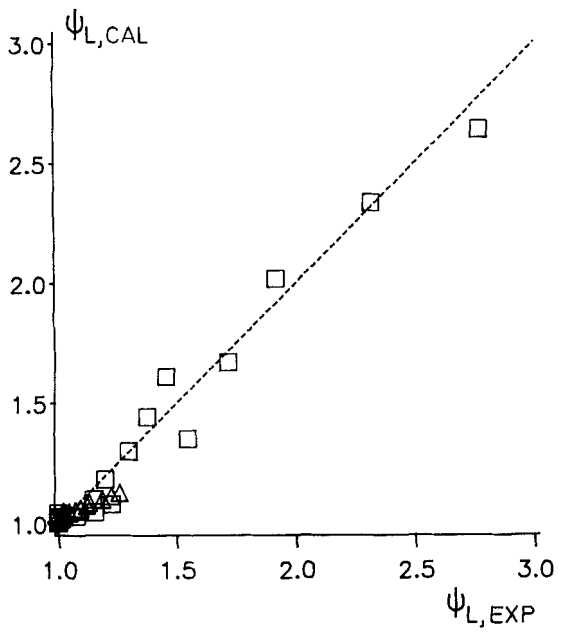


**Figure 6. Comparison of predicted and experimental pressure drops: symbols refer to Tables 2 to 4.**

The fluctuations of the estimates of $A$ are rather weak: an averaged value around 190 may be proposed. The fluctuations of $B$ are more important, but the latter parameter is not very accurately determined, because the turbulent contribution in the Ergun equation is rather weak in the range of low gas and liquid flow rates adopted in laboratory trickle-bed reactors.

The estimates of the minimum Reynolds number $Re_{min}$ are all very small (around 1). This is due to both the good effective wettability of porous particles and the small size of these particles. The small values of $Re_{min}$ imply that the experiments analyzed here were carried out under good wetting conditions, typically with a wetting efficiency ranging between 0.5 and 1 (see Figure 4, symbol □). The estimates of $Re_{min}$ reported in Table 2 indicate that the particle wettability is increased when α-methylstyrene is used in place of water or when smaller particles are used. In both cases, the energy necessary to wet the solid is reduced as indicated by the wetting criterion developed by Wijffels et al. (1974) (Eq. 23). These results will be further discussed when comparing the whole set of $Re_{min}$ estimates to this criterion.

*Nonporous Particles in Trickle-Bed Reactors.* The numerous studies considering these experimental operating conditions have been thoroughly reviewed (Gianetto et al., 1978; Smith et al., 1987). Among them, we will detail two especially interesting series of data. The first one, reported by Wijffels et al. (1974), consists of measurements of the wetting efficiency in a packing of glass spheres. Such data are rather scarce, because this type of experiment is much more difficult to achieve with nonporous particles. The second series of data was obtained more recently by Levec et al. (1986). These experiments consist of liquid holdup and pressure drop measurements in a packing of glass spheres. The essential characteristics of all these data are given in Table 3.

In both articles, the authors highlighted the influence of the solid wettability on the liquid flow hydrodynamics. They reported the existence of hysteresis phenomena based on whether the liquid flow rate is monotonously decreased or increased. Each of these two operating modes provokes the formation of different contact angles between the gas-liquid and liquid-solid interfaces. If the liquid flow rate is increased from one experiment to another, the liquid film progressively spreads over the initially dry solid. An "advancing" contact angle is formed. In the other case, a much smaller "receding" contact angle is formed. The difference between these two contact angles leads to strong differences between the two solid wettabilities. This should result in different minimum Reynolds numbers corresponding to these two operating modes. That is the reason two parametric values of $Re_{min}$ were adopted to fit our model on the hysteresis observed by Wijffels et al. (1974) for the solid wetting and by Levec et al. (1986) for the dynamic liquid holdup and the pressure drop.

The estimates of $Re_{min}$, $A$ and $B$ are given in Table 3 together with the sources of data. The agreement between predicted and experimental values is shown in Figures 4 to 6 (symbol Δ).

The $A$ and $B$ values are almost constant whatever the particle size is. They were assumed to be independent of the operating mode (decreasing or increasing flow rates). The coefficients of the Ergun equation indeed represent the influence of the packing structure and should not depend on the solid wettability.

The estimates of $Re_{min}$ are systematically larger for the data obtained under increasing liquid flow rates. This results in a systematically smaller wetting when adopting this operating mode. The hysteresis phenomena may thus be explained by differences between the advancing and receding contact angles, which in turn cause differences in the liquid flow texture, see Figures 7 and 8. A larger value of $Re_{min}$ (increasing flow rates) corresponds to a smaller wetting efficiency (Figure 7) (Wijffels et al., 1974) and to a smaller liquid holdup (Figure 8) (Levec et al., 1986). The values of $Re_{min}$ will be further discussed later on.

**Table 3. Parameter Estimates Corresponding to Nonporous Particles in Trickle-Bed Reactors**

| Reference | Symbols | Particle Dia. | Porosity | Liquid | $A$ | $B$ | $Re_{min}$ Decr. | $Re_{min}$ Incr. |
|---|---|---|---|---|---|---|---|---|
| Levec et al. (1986) | ▲ Δ | 0.3 cm | 0.38 | Water | 140 | 1.3 | 1.0 | 1.9 |
| Levec et al. (1986) | ▲ Δ | 0.3 cm | 0.38 | Water + Surfac. | 145 | 1.4 | 0.7 | 4.3 |
| Levec et al. (1986) | ▲ Δ | 0.6 cm | 0.38 | Water | 135 | 1.5 | 1.1 | 12.5 |
| Levec et al. (1986) | ▲ Δ | 0.3 cm | 0.38 | Water | 140 | 1.3 | 1.1 | 13.1 |
| Wijffels et al. (1974) | ▲ | 0.1 cm | 0.38 | Water | 140 | 1.3 | 0.3 | – |
| Wijffels et al. (1974) | ▲ Δ | 0.3 cm | 0.38 | Water | 140 | 1.3 | 2.4 | 16.2 |
| Wijffels et al. (1974) | ▲ | 0.5 cm | 0.38 | Water | 140 | 1.3 | 6.2 | – |
| Wijffels et al. (1974) | ▲ | 0.95 cm | 0.38 | Water | 140 | 1.3 | 6.7 | – |

* ▲, decreasing flow rate; Δ, increasing flow rate ($\langle Re_L \rangle = 0 - 150$; $\langle Re_G \rangle = 0 - 20$)

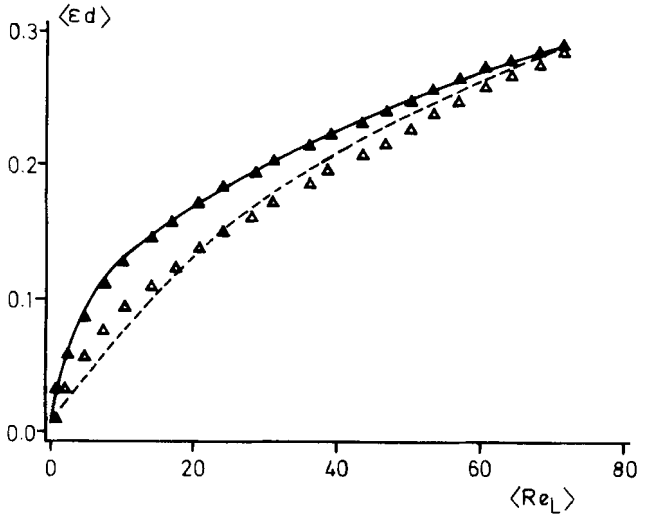


**Figure 7. Hysteresis phenomenon for the wetting efficiency reported by Wijffels et al. (1974) ($\langle Re_G \rangle = 0$; $d_p = 0.3$ cm).**

▲, decreasing flow rate; △, increasing flow rate.

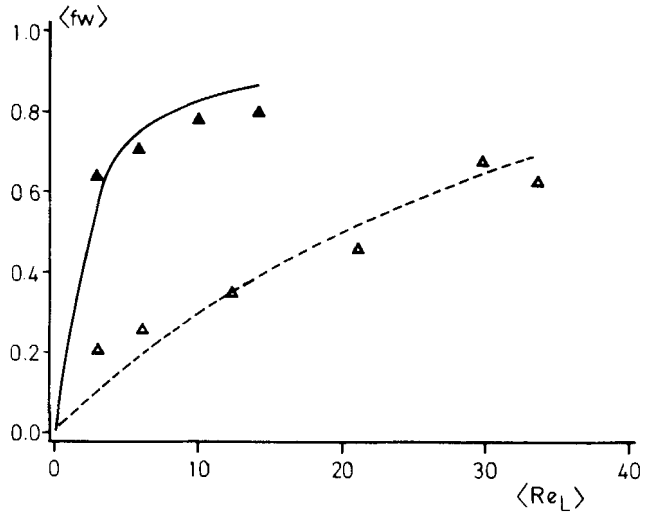


**Figure 8. Hysteresis phenomenon for the dynamic liquid holdup reported by Levec et al. (1986) ($\langle Re_G \rangle = 0$; $d_p = 0.3$ cm).**

▲, decreasing flow rate; △, increasing flow rate.

*Nonporous Particles in Gas-Liquid Absorption Columns.* These columns are usually operated countercurrently at high gas and/or liquid flow rates. The interactions between the two fluids are often important and cannot be neglected as we did in our model. This is especially true when the operating conditions are close to the flooding point. Some published data, however, report that they were obtained at sufficiently low fluid flow rates to neglect these interactions. Among these works, we will consider a series of data reported by Charpentier et al. (1968). This study consisted of measurements of the dynamic liquid holdup and pressure drop. It was carried out with different types of Raschig rings and different liquid properties. These characteristics are given in Table 4. To satisfy our assumption of low gas-liquid interactions, we will consider only the data obtained at a zero gas flow rate. Figures 4 to 6 show the fitting of these data (symbol ◇). Table 4 presents also the parameter estimates. Because of the similarity of the different particle shapes, we adopted a single set of $A$ and $B$ values for the whole set of data. These values are significantly smaller than the estimates obtained from packings classically used in trickle-bed reactors, such as spheres, granules, and cylinders. The estimate of $A$ equals 90, instead of 180 as proposed by Macdonald et al. (1979). This estimate is also considerably out of the range of values reported above for spheres and granules: 140–240. Actually, Raschig rings are hollow particles, part of whose internal surface cannot be geometrically accessed by the liquid, whatever the fluid flow rates are. This decrease of the static accessibility reduces the amount of liquid film covering the solid for a given liquid flow rate. This is accounted for in the Ergun equation by a decrease of coefficients $A$ and $B$.

The estimates of $Re_{min}$ reported in Table 4 increase, as the solid wettability is decreased either by a silicone coating or by replacing glass by polyethylene. $Re_{min}$ also increases with the equivalent diameter of the Raschig rings. A comparison between Table 4 (Raschig rings) and Table 3 (spheres) shows that the estimates of $Re_{min}$ are systematically larger for Raschig rings. The porosity is the main difference between these two types of packing: around 0.7 for Raschig rings and 0.4 for spheres.

## *Interpretation*

The fittings of our model based on the concept of "statistical hydrodynamics" on a large variety of experimental data are quite satisfying. This model gives a standard deviation of $5 \times 10^{-2}$ for the wetting efficiency $\langle f_w \rangle$ (Figure 4), $8 \times 10^{-3}$ for the dynamic liquid holdup $\langle \epsilon_d \rangle$ (Figure 5), and $6 \times 10^{-2}$ for the pressure drop $\psi_L$ (Figure 6). This means that, in the range of investigated data, the relative error is of the order of 5-6% for the three variables considered here. This represents a quantitative improvement if we compare our results to correlations

**Table 4. Parameter Estimates Corresponding to Nonporous Particles in Gas-Liquid Absorption Columns (Charpentier et al., 1968)**

| Symbol | Particle Dia. | Porosity | Solid | Liquid | $A$ | $B$ | $Re_{min}$ |
|---|---|---|---|---|---|---|---|
| ◇ | 0.21 cm | 0.70 | Glass | Water | 90 | 1.1 | 15.6 |
| ◇ | 0.44 cm | 0.67 | Glass | Water | 90 | 1.1 | 32.8 |
| ◇ | 0.44 cm | 0.67 | Glass | Water + Saccharose | 90 | 1.1 | 0.7 |
| ◇ | 0.44 cm | 0.67 | Glass | Water + Isopropanol | 90 | 1.1 | 13.5 |
| ◇ | 0.44 cm | 0.69 | Glass + Silicone Coat. | Water | 90 | 1.1 | 9.5 |
| ◇ | 0.87 cm | 0.73 | Polyethylene | Water | 90 | 1.1 | 272 |

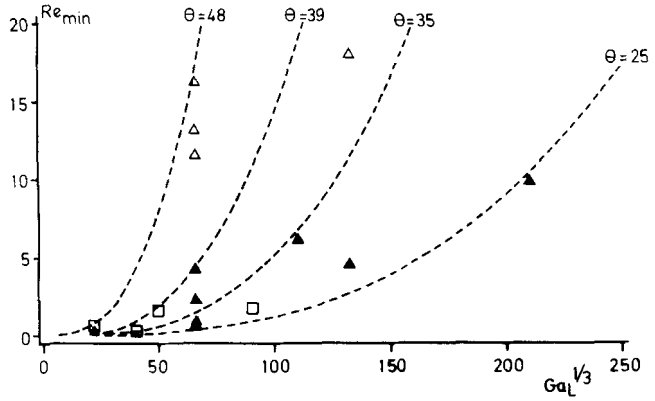


**Figure 9. $Re_{min}$ estimates and prediction of the Wijffels criterion for a packing void fraction of 0.4.**

△, glass sphere, increasing flow rate; ▲, glass sphere, decreasing flow rate; □, porous granules.

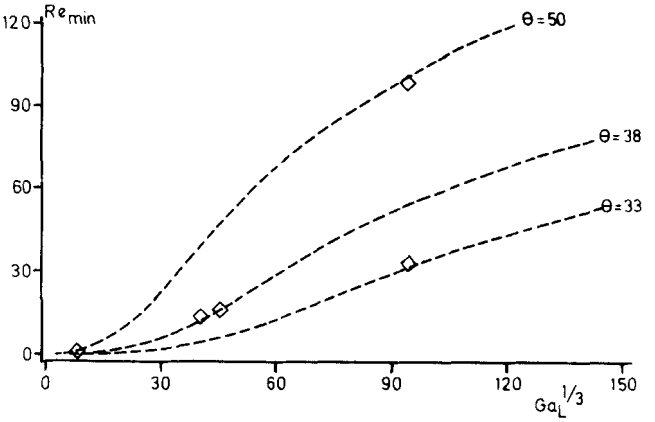


**Figure 10. $Re_{min}$ estimates and prediction of the Wijffels criterion for a packing void fraction of 0.7.**

◇, Raschig rings.

that were tested against a similar variety of packing properties (for example, the correlation proposed by Sáez and Carbonell, 1985). We must also point out that our model correlates simultaneously the pressure drop, the dynamic liquid holdup, and the wetting efficiency, whereas previous models described the first two quantities only.

A part of this improvement is probably achieved by adopting different sets of parameters $A$, $B$, and $Re_{min}$ for different packings, fluids and operating modes. As a matter of fact, this was the only way to perform a detailed analysis of the influence of the two types of packing properties: the texture ($A$ and $B$) and the wettability ($Re_{min}$).

Coefficients $A$ and $B$ fluctuated rather widely since the packing types varied with particle diameters ranging from 0.1 to 0.95 cm, and bed porosities from 0.36 to 0.73. These fluctuations, however, are much less important if we consider a single type of packing. $A$ and $B$ are close to 150 and 1.4 for nonporous, spherical particles (glass spheres); close to 200 and 5 for porous, nonspherical particles (granules, cylinders) and close to 90 and 1.1 for hollow particles as Raschig rings. The sphericity of the particles seems to play an important role: it may modify the homogeneity of the packing. A decrease in the sphericity causes an increase of the packing tortuosity, and, in turn, a decrease of the absolute permeabilities (the inverses of $A$ and $B$).

The packing structure is undoubtedly an essential parameter determining the values of coefficients $A$ and $B$. In the absence of clear information on this sturcture, the coefficients of the Ergun equation will remain empirical parameters to be deduced from experiments.

The wetting criterion of Wijffels et al. (1974), described above, allows an easy interpretation of variations of the $Re_{min}$ estimates. According to Eq. 23, the minimum Reynolds number depends on four quantities characterizing the fluid and packing properties: the packing void fraction $\epsilon$, the Galileo number $Ga_L$, the Eötvos number $Eo_L$, and the modified Eötvos number $Eo_S$.

$Re_{min}$ should also be a function of the pressure drop $\psi_L$, but this does not vary significantly for most of the data investigated. Furthermore, for these data, the term in $Re_{min}^2$ (kinetic energy) in Eq. 23 is relatively small so that the minimum Reynolds number depends mainly on the ratio $Eo_L/Eo_S$, that is, the contact angle $\theta$. To account for these three dependencies ($\epsilon$, $Ga_L$, and $\theta$), the estimates of $Re_{min}$ are graphically represented vs. $Ga_L^{1/3}$ ($\propto d_p$) separately for two values of $\epsilon$: 0.4 for packings of spheres and granules (Figure 9), and 0.7 for packings of hollow particles (Figure 10). The symbols are those used in Tables 2 to 4. The Wijffels criterion is also reproduced on these figures for different values of the contact angle $\theta$. We note that the influence of $Ga_L$ was determined by varying the particle diameter $d_p$ and keeping constant the properties of the fluid (assumed to be water). Mean values of the Ergun constants $A$ and $B$ were taken for the calculations required by Eq. 23: 150 and 1.4 for packings of spheres ($\epsilon = 0.4$), and 90 and 1.1 for packings of hollow particles ($\epsilon = 0.7$).

Most of the data analyzed here were obtained with the same material: glass. The contact angle $\theta$ should thus be reproducible at least for the same operating mode. Actually, despite some important scatter in the $Re_{min}$ estimates, the corresponding contact angles lie in rather narrow ranges. The receding contact angles (decreasing liquid flow rates) range from 25° to 35° in Figure 9, and from 33° to 38° in Figure 10. For this range of $\theta$ values, the critical surface tension $\sigma_c$ defined by

$$\sigma_c = \sigma_L \frac{1+\cos\theta}{2} \tag{32}$$

ranges from 63 to 67 g/s$^2$. These results are close to the data reported by Shi and Mersmann (1985). In Figure 10, one estimate is situated somewhat out of the range. It corresponds to a contact angle close to 50°. One may observe that this value of $Re_{min}$ corresponds to silicone-coated glass particles, the surface of which is undoubtedly more difficult to wet (Table 4).

The advancing contact angles (Figure 9) range from 39° to 48°. These values are logically larger than the receding ones. They are close to 49°, which is a value reported by Schröder et al. (1982) using the "deposited droplet" technique. This measurement of a static contact angle may be considered to be rather similar to the increasing flow rate technique. The liquid droplet is indeed deposited and progressively spreads on the initially dry solid surface.

The influence of porosity and particle size is shown in Figures 9 and 10. For small porosities ($\epsilon \approx 0.4$), $Re_{min}$ is clearly a cubic function of the particle diameter $d_p$ (or $Ga_L^{1/3}$) in Figure 9. This corresponds to the case of Eq. 31. For larger porosities ($\epsilon \approx 0.7$), this relationship is still valid for small values of $Ga_L$ (see Figure 10). For higher values, $Re_{min}$ tends to progress to a constant value independent of the particle size. This asymptotic limit is determined by Eq. 29.

## Conclusions

The main objective of this work is to provide some new insights into the intricate mechanisms and packing properties ruling the liquid flow distribution and the hydrodynamics in trickle beds. The properties of the packing vary in such a complex manner within the column that they have to be considered as random variables, whose variations are described by probability distributions. We think that the concept of statistical hydrodynamics accounts for this complex phenomena. The modeling relies on two levels of description.

The local or microscopic level corresponds to the smallest volume of an elementary cell, whose averaged geometrical properties are representative of the whole packing texture. With statistically homogeneous packings usually used in trickle flow columns, the characteristic length of this cell is close to the particle size. The hydrodynamics at this level is described by a constitutive equation such as the Ergun equation.

This work adopted a higher level of modeling that accounts for the influence of liquid flow maldistribution. This phenomenon is controlled mainly by the solid wettability. Its characteristic length is usually much larger than the particle size. This defines the macroscopic level at which averaged hydrodynamic quantities represent the whole packing.

The solid wettability may be characterized by the minimum Reynolds number $Re_{min}$ necessary to wet the solid surface. At given gas and liquid flow rates, this parameter determines the state of segregation of the gas-liquid flow: rivulets or films. This, in turn, determines the relative permeabilities of the packing. The different estimates of $Re_{min}$, based on a large variety of experimental data, are well correlated by the wetting criterion of Wijffels et al. (1974). The hysteretic behavior of trickle beds may be explained by a modification of the liquid flow texture caused by distinct values of the contact angle (and thus of $Re_{min}$) depending whether the liquid flow rate is monotonously increased or decreased.

The correlations of $\psi_L$, $\langle \epsilon_d \rangle$ and $\langle f_w \rangle$ proposed in this article give accuracies as good or even better than those obtained with previous correlations with the advantage of correlating simultaneously three quantities rather than two as achieved in previous works.

## Notation

$A$ = constant in the Ergun equation (laminar contribution)
$B$ = constant in the Ergun equation (turbulent contribution)
$c$ = constant introduced in the probability distribution (Eq. 10)
$C_e$ = constant defined by Eq. 23
$d$ = constant introduced in the probability distribution (Eq. 10)
$d_p$ = particle diameter, cm
$Eo_L$ = Eötvos number in the liquid phase defined by $\rho_L g d_p^2/\sigma_L$
$Eo_S$ = modified Eötvos number defined by $\rho_L g d_p^2/E_s$
$E_S$ = surface energy necessary to create a liquid trickling film, $g/s^2$
$f_w$ = wetting efficiency
$g$ = acceleration of gravity, $cm/s$
$Ga_G$ = Galileo number in the gaseous phase defined by $d_p^3\rho_G^2 g/\mu_G^2$
$Ga_L$ = Galileo number in the liquid phase defined by $d_p^3\rho_L^2 g/\mu_L^2$
$k_G$ = relative permeability in the gaseous phase
$k_L$ = relative permeability in the liquid phase
$p(Re_{L,i})$ = probability to observe a local liquid flowrate characterized by a Reynolds number $Re_{L,i}$
$P_G$ = pressure in the gaseous phase, $g/cm \cdot s^2$
$P_L$ = pressure in the liquid phase, $g/cm \cdot s^2$
$Re_G$ = gas Reynolds number defined by $\rho_G u_G d_p/\mu_G$
$Re_L$ = liquid Reynolds number defined by $\rho_L \mu_L d_p/\mu_L$
$Re_{max}$ = maximum Reynolds number causing a local flooding
$Re_{min}$ = minimum Reynolds number ensuring a local wetting
$u_G$ = gas superficial velocity, cm/s
$u_L$ = liquid superficial velocity, cm/s
$x$ = axial coordinate, cm

### Greek letters

$\alpha$ = constant defined by Eq. 24
$\epsilon$ = packing void fraction
$\epsilon_d$ = dynamic liquid holdup
$\epsilon_S$ = static liquid holdup
$\theta$ = contact angle
$\mu_G$ = gas viscosity, g/cm•s
$\mu_L$ = liquid viscosity, g/cm•s
$\rho_G$ = gas density, $g/cm^3$
$\rho_L$ = liquid density, $g/cm^3$
$\sigma_L$ = liquid surface tension, $g/s^2$
$\sigma_c$ = critical surface tension, $g/s^2$
$\psi_L$ = dimensionless pressure drop of liquid phase including gravity effects

### Other symbols

$i$ = local or microscopic variable in channel $i$
$\langle \bullet \rangle$ = macroscopic variable defined over the whole packing

## Literature Cited


Bankoff, S. G., "Stability of Liquid Flow Down a Heated Inclined Plane," *Int. J. Heat Mass Transfer*, **14**, 377 (1971).

Brenner, H., "Dispersion Resulting from Flow through Spatially Periodic Porous Media," *Phil. Trans. Royal Soc. London*, **297**, 81 (1980).

Carbonell, R. G., and S. Whitaker, "Heat and Mass Transfer in Porous Media," *Fundamentals of Transport in Porous Media*, J. Bear and Y. Corapcioglu, eds., p. 121, Martinus Nijhoff, Dordrecht (1984).

Charpentier, J. C., C. Prost, W. van Swaaij, and P. Le Goff, "Etude de la Rétention de Liquide dans une Colonne à Garnissage Arrosé à Cocourant et à Contrecourant de Gaz-Liquide: Représentation de sa Texture par un Modèle à Films, Filets et Gouttes," *Chimie et Industrie-Génie Chimique*, **99**, 803 (1968).

Christensen, G., S. J. McGovern, and S. Sundaresan, "Cocurrent Downflow of Air and Water in a Two-Dimensional Packed Column," *AIChE J.*, **32**, 1677 (1986).

Chu, C. F., and K. M. Ng, "Model for Pressure Drop Hysteresis in Trickle Beds," *AIChE J.*, **35**, 1365 (1989).

Colombo, A., G. Baldi, and S. Sicardi, "Liquid-Solid Contacting Efficiency in Trickle-Bed Reactors," *Chem. Eng. Sci.*, **31**, 1101 (1976).

Crine, M., "Contribution Expérimentale et Théorique à la Connaissance du Fonctionnement des Réacteurs Gas-Liquide à Lit Catalytique Fixe Arrosé," Thèse de Doctorat en Sciences Appliquées, Université de Liège, Liège (1978).

Crine, M., *Hydrodynamique Statistique des Écoulements Gaz-Liquide dans les Colonnes à Garnissages: Théorie et Expérience*, Ed. Cebedoc, Liège (1988).

Crine, M., P. Marchot, and G. L'Homme, "Mathematical Modeling of the Liquid Trickling Flow through a Packed Bed Using the Percolation Theory," *Comp. Chem. Eng.*, **3**, 629 (1979).
Crine, M., and P. Marchot, "Les Écoulements Gaz-Liquide à Cocourant Vers le Bas en Lit Granulaire Fixe, Première Partie: Description des Structures d'Écoulement du Liquide," *Entropie*, **102**, 28 (1981).
Crine, M., and P. Marchot, "Les Écoulements Gaz-Liquide á Cocourant Vers le Bas en Lit Granulaire Fixe, Deuxième Partie: Modèle Stochastique de l'Ecoulement du Liquide," *Entropie*, **102**, 37 (1981).
Crine, M., M. Schlitz, and L. Vandevenne, "A Partial Wetting Model for Aerobic Trickling Filters," *Chem. Eng. J.*, **46**, B59 (1991).
Dankworth, D. C., I. G. Kevrekidis, and S. Sundaresan. "Dynamics of Pulsing Flow in Trickle Beds," *AIChE J.*, **36**, 605 (1990).
Ergun, S., "Fluid Flow through Packed Columns," *Chem. Eng. Prog.*, **48**, 89 (1952).
Gianetto, A., G. Baldi, V. Specchia, and S. Sicardi, "Hydrodynamics and Solid-Liquid Contacting Effectiveness in Trickle-Bed Reactors," *AIChE J.*, **24**, 1087 (1978).
Grosser, K., R. G. Carbonell, and S. Sundaresan, "Onset of Pulsing in Two-Phase Cocurrent Downflow through a Packed Bed," *AIChE J.*, **34**, 1850 (1988).
Hartley, D. E., and W. Murgatroyd, "Criteria for the Breakup of Thin Liquid Layers Flowing over a Solid Surface," *Int. J. Heat Mass Transfer*, **7**, 1003 (1964).
Herskowitz, M., "The Performance of Trickle-Bed Reactors," PhD Thesis, Univ. of California, Davis (1978).
Hobler, T., "Minimum Zraszania Pouierzehni," *Chem. Stosow.*, Ser. B., **1**, 145 (1964).
Hoek, P. J., "Small-Scale and Large-Scale Liquid Maldistribution in Packed Columns," *Chem. Eng. Res. Des.*, **64**, 431 (1986).
Jaynes, E. T., "The Maximum Entropy Principle," *The Maximum Entropy Formalism*, R. D. Levine and M. Tribus, eds., p. 15, MIT Press, Cambridge, MA (1979).
Levec, J., A. E. Sáez, and R. G. Carbonell, "The Hydrodynamics of Trickling Flow through Packed Beds: 2. Experimental Observations," *AIChE J.*, **32**, 369 (1986).
Macdonald, I. F., M. S. El-Sayed, K. Mow, and F. A. Dullien, "Flow through Porous Media: the Ergun Equation Revisited," *Ind. Eng. Chem. Fundam.*, **18**, 199 (1979).
Marchot, P., "Description Stochastique de L'Écoulement Ruisselant dans les Lits Fixes," Thèse de Doctorat en Sciences Appliquées, Université de Liège (1988).
Marchot, P., M. Crine, and G. L'Homme, "Two-Phase Flow through a Packed Bed: a Stochastic Model Based on Percolation Concepts," *Chem. Eng. J.*, **36**, 141 (1987).
Mata, A. R., and J. M. Smith, "Oxidation of Sulfur Dioxide in a Trickle-Bed Reactor," *Chem Eng. J.*, **22**, 229 (1981).
Matheron, G., "Structure et Composition des Perméabilités, "*Inst. Franç. du Pétrole*, **21**, 564 (1966).
Mikielewicz, J., and J. R. Moszynski, "Minimum Thickness of a Liquid Film Flowing Vertically Down a Solid Surface," *Int. J. Heat Mass Transfer*, **19**, 771 (1976).
Oger, L., G. Gauthier, C. Leroy, J. P. Hulin, and E. Guyon, "Hétérogénéités et Longueurs Caractéristiques dans les Milieux Poreux," *Entropie*, **152**, 29 (1989).
Puranik, S. S., and A. Vogelpohl, "Effective Interfacial Area in Irrigated Columns," *Chem. Eng. Sci.*, **29**, 501 (1974).
Rao, V. G., and A. A. Drinkenburg, "A Model for Pressure Drop in Two-Phase Gas-Liquid Downflow through Packed Columns," *AIChE J.*, **31**, 1010 (1985).
Sáez, A. E., and R. G. Carbonell, "Hydrodynamic Parameters for Gas-Liquid Cocurrent Flow in Packed Beds," *AIChE J.*, **31**, 52 (1985).
Sáez, A. E., R. G. Carbonell, and J. Levec, "The Hydrodynamics of Trickling Flow in Packed Beds: 1. Conduit Models," *AIChE J.*, **32**, 353 (1986).
Scheidegger, A. E., *The Physics of Flow through Porous Media*, Univ. of Toronto Press, Toronto (1974).
Schröder, J. J., U. Pohl, and A. Horsthemke, "Minimum Flow Rates and Rewetting-Rates of Falling Films," Int. Heat Transfer Conf., U. Grigull, E. Hahne, and K. Stephan, eds., p. 83, München (1982).
Shah, Y. T., *Gas-Liquid-Solid Reactor Design*, McGraw-Hill, New York (1979).
Shi, M. G., and A. Mersmann, "Effective Interfacial Area in Packed Columns," *Ger. Chem. Eng.*, **8**, 87 (1985).
Sicardi, S., G. Baldi, V. Specchia, I. Mazzarino, and A. Gianetto, "Packing Wetting in Trickle-Bed Reactors: Influence of the Gas Flow Rate," *Chem. Eng. Sci.*, **36**, 226 (1981).
Slattery, J. C., *Momentum, Energy and Mass Transfer in Continua*, McGraw-Hill, New York (1972).
Smith, D. N., G. J. Stiegel, and J. A. Ruether, *Modeling Three-Phase Reactor Systems*, Vol. 6, p. 535, Gulf Publishing, Houston (1987).
Specchia, V., and G. Baldi, "Pressure Drop and Liquid Holdup for Two-Phase Cocurrent Flow in Packed Beds," *Chem. Eng. Sci.*, **32**, 515 (1977).
Whitaker, S., "Advances in the Theory of Fluid Motion in Porous Media," *AIChE J.*, **61**, 14 (1969).
Wijffels, J. B., J. Verloop, and F. J. Zuiderweg, "On the Wetting of Catalyst Particles Under Trickle-Flow Conditions," ACS Ser. 133, *Chem. Reaction Eng. II*, p. 151 (1974).
Zanotti, F., and R. G. Carbonell, "Development of Transport Equations for Multiphase Systems: I. General Development for Two-Phase Systems," *Chem. Eng. Sci.*, **39**, 263 (1984).

*Manuscript received Dec. 19, 1990, and revision received Nov. 4, 1991.*